Journal of The Electrochemical Society, 155 (6) H363-H368 (2008)
0013-4651/2008/155(6)/H363/6/$23.00 © The Electrochemical Society

Properties of Ge Films Grown Through Inductively Coupled Plasma Chemical Vapor Deposition on SiO_2 Substrates

Ming-Jui Yang,[a,b] Chao-Hsin Chien,[a,b,z] Chih-Yen Shen,[b] and Tiao-Yuan Huang[a]

[a]*Institute of Electronics, National Chiao Tung University, Hsin-Chu 300, Taiwan*
[b]*National Nano Device Laboratories, Hsin-Chu, 30078 Taiwan*

In this study, we investigated the physical and electrical characteristics of Ge polycrystalline films deposited directly onto SiO_2-covered substrates using inductively coupled plasma chemical vapor deposition (ICP-CVD). The pure Ge films that we deposited at a relatively low temperature of 300°C exhibited the same cubic structure, with primarily (111), (220), and (311) orientations identified from X-ray diffraction patterns, as those deposited at 400°C. The use of such a low temperature not only prevented the plasma window of the chamber from overheating but also allowed crack-free, thicker films to be deposited more easily. The ability to deposit Ge films on SiO_2 was closely linked to the hydrogen etching effect, as evidenced by the results obtained using X-ray photoelectron spectroscopy. Although the crystalline characteristics of the low-temperature as-deposited Ge films were somewhat poorer than those obtained at 400°C, subsequent furnace annealing and rapid thermal annealing with a SiN_x capping layer improved the crystalline quality significantly. These results, taken together with studies of the surface morphologies and dopant activation of the recrystallized Ge films, suggest that ICP-CVD might be a simple, powerful and reliable approach for the fabrication of polycrystalline Ge thin film transistors.
© 2008 The Electrochemical Society. [DOI: 10.1149/1.2901885] All rights reserved.

Manuscript submitted January 2, 2008; revised manuscript received February 20, 2008. Available electronically April 8, 2008.

Germanium is attracting increasing attention because of its wide applications in ultralarge-scale integration and nanotechnology. Ge/Si and SiGe/Si heterostructures have been used in high-performance devices because of their higher electron and hole mobilities relative to those of Si.[1-5] Three-dimensional Ge islands formed on Si surfaces through solid-phase epitaxy have great potential for use in fabricating nanostructures.[6] In addition, Ge on insulators are especially desired for the preparation of extremely high-performance metal oxide silicon field-effect transistors exhibiting sufficiently low leakage currents.[7,8] For thin-film transistor (TFT) applications, poly-Ge deposited using molecular beam epitaxy has been applied to replace the poly-Si channel because poly-Ge exhibits a higher field-effect mobility.[9] Successful Ge thin-film deposition directly on SiO_2 substrates using chemical vapor deposition (CVD) techniques has not been demonstrated previously, however, because an extremely long incubation time is required.[10-16] Nevertheless, CVD has the advantage of uniformity control which is highly important in the larger dimension substrates and mass production, relative to such techniques as sputtering[17] and e-gun deposition.[18,19]

In this paper, we report the physical and electrical properties of Ge films deposited at 300°C using inductively coupled plasma (ICP)-CVD techniques. In a previous study, we demonstrated that the deposition could be performed at 400°C,[20] but such a high temperature caused overheating of the plasma windows (the top plate for plasma generation) and led to the formation of an abundance of particles, which is obviously detrimental to the quality of the Ge films. Increasing the cooling interval from run to run could relieve the overheating of the plasma window, but it would decrease the throughput of the production. Therefore, in this study we lowered the deposition temperature to 300°C to prevent overheating of the plasma window and determined the properties of the resultant thin films. In addition, we found that the mechanism of deposition was related to a hydrogen etching effect from the plasma, rather than a gas-phase reaction or carbon contamination. To enhance the grain size and quality of the as-deposited Ge films, we performed a recrystallization process using a SiN_x capping layer. Finally, we investigated the electrical characteristics of the n- and p-doped polycrystalline Ge thin films.

Experimental

After standard cleaning, 550 nm thick SiO_2 layers were thermally grown on p-type Si(100) wafers in a furnace. Subsequently, the oxidized wafers were transferred to a process chamber of an ICP-CVD system. Prior to depositing the first Ge film, the reaction chamber was cleaned using a CF_4/O_2 mixture at 350°C. Ge films were then deposited using an ICP-CVD system at a deposition temperature of either 300 or 400°C. The process pressure of the reaction chamber was 50 mTorr; the gas species were GeH_4 (3 sccm), H_2 (150 sccm), and Ar (30 sccm). The plasma generation radio frequency (rf) power from an ICP generator (13.56 MHz) was 500 W; no additional bottom rf power supply was used. Simultaneously, the other experiment about plasma treatment using only hydrogen plasma was also performed on the oxidized wafer to observe the H_2 etching effect. A SiN_x layer, deposited using a SiH_4/NH_3 mixture at 375°C, was also deposited using the ICP-CVD system to cap the Ge films prior to their recrystallization to reduce the extent of any reactions with residual oxygen. After deposition, the Ge films were recrystallized in the furnace and in a rapid thermal annealing (RTA) system to enhance the crystalline properties of the low-temperature-grown Ge films. Dopant activation of the Ge films, which was conducted in the RTA system at various temperatures under an N_2 atmosphere, was followed by the implantation of boron and phosphorus using a dosage of 5×10^{15} cm^{-2} at 50 and 130 KeV, respectively. Scanning electron microscopy (SEM) was used to identify the physical thickness of the Ge films and, hence, to calculate the rate of deposition. X-ray photoelectron spectroscopy (XPS) and Auger electron spectroscopy (AES) were employed to detect the composition and contamination of the deposited Ge films. The crystalline properties of the Ge films were evaluated through X-ray diffraction (XRD) measurements. Atomic force microscopy (AFM) was used to determine the film roughness. The sheet resistances of the activated Ge films were measured using a four-point probe system.

Results and Discussion

Effect of deposition temperature.— Plasma-enhanced CVD and high-density plasma CVD systems were designed for applications requiring low temperatures. Although high substrate temperatures can enhance the quality of the as-deposited film, they should not be too high so that they have a negative effect on processing. During deposition, the top plate for plasma generation is hot; a substrate at higher temperature will lead to a hotter plasma window. In addition, the coated films on the top plate might become cracked as a result of overheating and might create many particles on the deposited Ge films. Although increasing the cooling interval can prevent these phenomena from occurring, the throughput would decrease accordingly, which would not be favorable for mass production. To reduce the overheating of the plasma window, we sought to lower the depo-

[z] E-mail: chchien@mail.ndl.org.tw

Downloaded on 2014-04-25 to IP 140.113.38.11 address. Redistribution subject to ECS terms of use (see ecsdl.org/site/terms_use) unless CC License in place (see abstract).

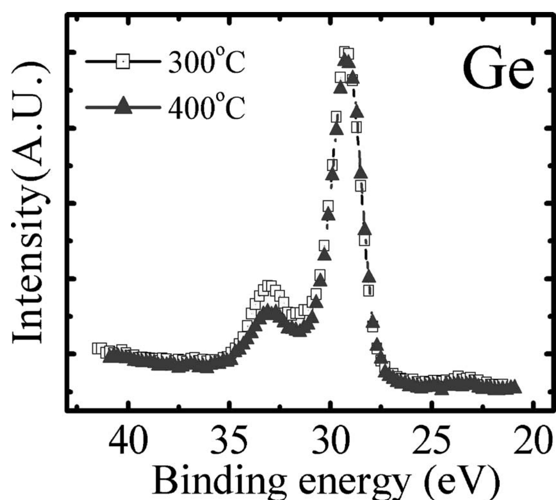

Figure 1. XPS measurements performed at the Ge 3d level spectrum revealing the surface conditions of the as-grown Ge films deposited onto SiO_2 substrate at 300 and 400°C. The comparative data of the Ge films deposited at 400°C were extracted from Ref. 20.

sition temperature to 300°C. Figure 1 displays XPS spectra of the as-grown Ge films deposited at 300 and 400°C. Consistent with our previous findings,[20] a very sharp Ge peak was clearly evident for each sample at a binding energy of 29.2 eV, with a small shoulder at higher binding energy, which we attribute to the formation of surface GeO_2 through oxidation when the sample was exposed to air. The AES profile of the Ge film deposited at 300°C (Fig. 2) confirmed that the oxygen atoms were present on the surface and not incorporated into the bulk: signals for O and C atoms both appeared close to the surface, but their intensity decreased abruptly thereafter. We obtained a similar result in our previous study of a Ge film deposited at 400°C.[20] According to these XPS and AES data, we believe that very pure Ge films can be deposited directly onto SiO_2-covered substrates at 300°C. The major drawback of performing deposition at such a low temperature was that the intensity of theGeO_2 peak was slightly stronger. We suspect that this phenomenon might be related to the formation of a thick surface-oxidized GeO_2 layer, which formed over the surface because of the poorer crystallinity of the low temperature-grown Ge film.

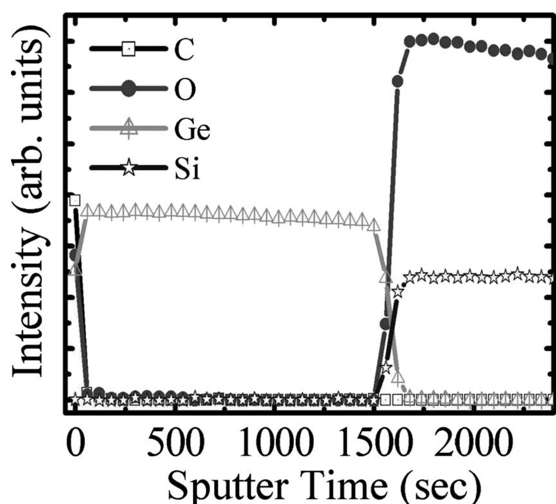

Figure 2. AES depth profiles of a Ge film deposited onto a SiO_2 substrate at 300°C.

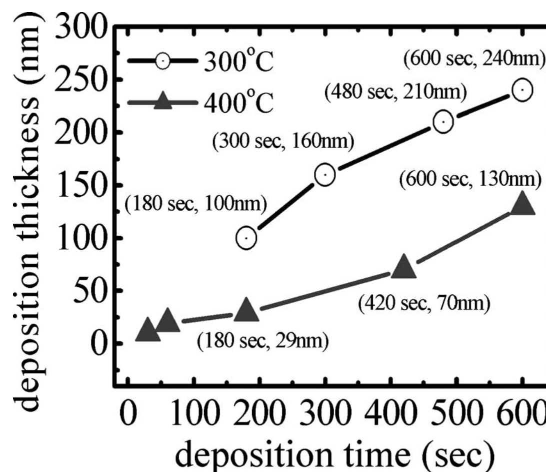

Figure 3. Ge film thickness (by SEM measurements) plotted as a function of the deposition time at 300 and 400°C. The comparative data of the Ge films deposited at 400°C were extracted from Ref. 20.

Figure 3 provides a comparison of the film thicknesses obtained at various deposition times and temperatures. A faster deposition rate $(24\ nm\ min^{-1})$ occurred for the sample deposited at 300°C, presumably because of a lower migration rate and a lower desorption rate of the Ge radicals on the surface at lower temperature. From XRD analyses (Fig. 4), we found that the sample deposited at 300°C possessed the same cubic structure, but with a smaller grain size (ca. 13.9 nm), as that deposited at 400°C (ca. 16.7 nm). Nevertheless, the faster deposition rate resulted in a Ge film of poorer crystallinity, but the recrystallization process could be used to enhance the crystallinity of the deposited Ge film (see the next section).

Mechanism of Ge film deposition.— No previous reports have described the successful deposition of Ge thin films on SiO_2 substrates using CVD techniques because of the extremely long incubation times required.[12-14,21,22] In our recent report,[20] we noted that the deposition of Ge onto SiO_2 substrates in an ICP-CVD system can be achieved with nearly no incubation time. We speculated that this result might be because the high density of H radicals will slightly etch the SiO_2 surface and partially reduce SiO_2 groups into Si or SiO_x units. Those exposed Si bonds on the surface could act as nucleation sites enhancing the probability of adsorption of Ge at-

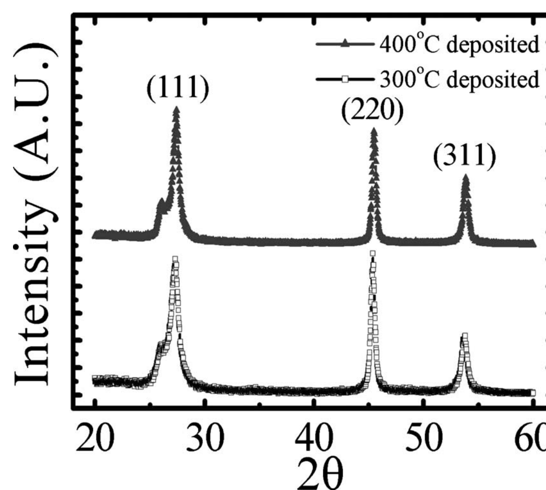

Figure 4. XRD patterns of the as-grown Ge films of ca. 150 nm thickness deposited onto SiO_2 substrates at 300 and 400°C.

Downloaded on 2014-04-25 to IP 140.113.38.11 address. Redistribution subject to ECS terms of use (see ecsdl.org/site/terms_use) unless CC License in place (see abstract).

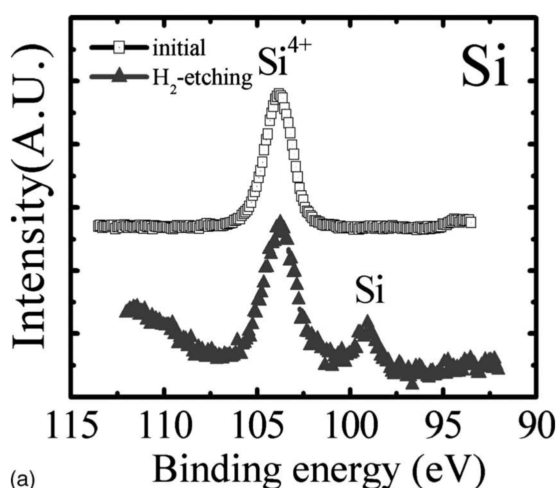

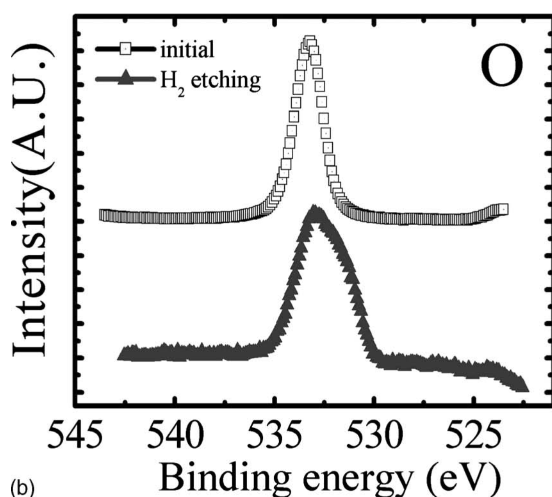

Figure 5. XPS spectra revealing the status of the (a) Si and (b) O atoms of an oxidized wafer before and after etching with H_2 plasma.

oms. Our hypothesis was based on two factors: (*i*) A previous paper reported that feeding SiH_4 gas into the chamber prior to deposition helps to form the nucleation sites on the SiO_2 surface, which considerably reduces the incubation time for the following Ge deposition.[15] (*ii*) Hydrogen etching effects have been observed previously in other plasma systems,[23,24] with the hydrogen radicals' etching of the SiO_2 surface resulting in the presence of the additional Si peak in XPS spectrum. Unlike other CVD systems, radicals of high energy can be generated during high-density plasma CVD, such as in ICP and electron cyclotron resonance CVD systems. The sheath layer would accelerate these radicals, such that slight etching of the sample surface would occur even in the absence of a bottom rf bias. To prove our hypothesis, we performed an etching test using H_2 plasma in our ICP-CVD system. The oxidized wafer was transferred to the process chamber and treated with H_2 plasma at 300°C for 30 s under an rf power of 500 W; no additional bottom rf power was applied. Because hydrogen atoms are so small, it is not easy to generate a stable plasma at low pressure; thus, we increased the process pressure from 10 to 50 mTorr and fed Ar gas into the chamber during the processing to overcome this problem. Figure 5 displays XPS spectra of the samples prepared with and without H_2 etching. From Fig. 5a, we observe a clear Si^{4+} peak for both samples, but an additional Si peak appeared in the spectrum of the sample obtained after H_2 plasma etching, which is consistent with previous findings.[23] In addition, the signal for the O atoms (i.e., for SiO_2 and SiO_x units) was broadened for the sample subjected to H_2

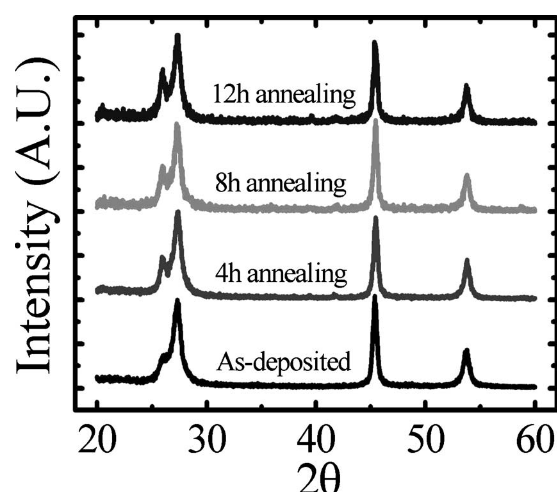

Figure 6. XRD patterns of the as-deposited Ge film without capping SiN_x layer and of the samples obtained after recrystallization in a furnace at 400°C for various lengths of time. The thicknesses of the Ge films were ca. 160 nm.

plasma etching, as shown in Fig. 5b, suggesting that the additional Si and SiO_x bonds that were created after H_2 plasma etching acted as nucleation sites for subsequent deposition of Ge atoms, which is consistent with our hypothesis.

Recrystallization of the as-deposited Ge film.— Although the Ge films could be deposited successfully at 300°C, they exhibited poor crystallinity. To enhance the qualities of the as-deposited Ge films, we utilized furnace and RTA methods to recrystallize them. Figure 6 displays XRD spectra of the as-deposited Ge film and the resultant samples after recrystallization at 400°C for various times in the furnace system under a N_2 ambient. We observe three main peaks corresponding to cubic (111), (220), and (311) orientations, respectively. As the annealing time increased, the mean grain size of recrystallized Ge films increased, suggesting that the quality of Ge films had improved. After recrystallization for 4 h, the grain sizes for the (111), (220), and (311) orientations, calculated roughly using Scherrer's formula ($D = 0.9\lambda/B \cos \Theta$), were 10.3, 19.1, and 13.9 nm, respectively. The mean grain size (ca. 14.4 nm) was slightly larger than that in the as-deposited Ge film. Accordingly, we have determined that pure Ge films can be deposited at a lower substrate temperature of 300°C and then the quality of the as-deposited film can be enhanced through recrystallization. We noted, however, that an additional peak near (111), which we assign to GeO_x species, emerged in the XRD spectra when the samples were annealed for >4 h. This phenomenon might be caused by the residual oxygen in the furnace, which would react with the Ge film to form GeO_x during longer annealing processes. When we increased the annealing temperature to 500°C, parts of the Ge film peeled off as a result of the decomposition of GeO_x after 1 h of annealing. To eliminate the formation of GeO_x during recrystallization, we capped a SiN_x layer of ca. 50 nm thickness over the Ge film to prevent it from reacting directly with residual oxygen. This SiN_x layer suppressed the intensity of the GeO_x peak dramatically after a long-duration, higher-temperature recrystallization (Fig. 7). The average grain size of the recrystallized Ge films featuring a SiN_x capping layer increased to ca. 16.7 nm, significantly larger than those for the uncapped samples. We also employed the RTA system in an attempt to enhance the crystallinity of the Ge films within a shorter time. Figure 8 displays XRD spectra of the Ge films that we recrystallized in the RTA system at various recrystallization temperatures and times. We observed that the polycrystalline cubic structure was retained after RTA treatments and that the grain size increased on increasing the annealing time or temperature. Moreover, the weak

Downloaded on 2014-04-25 to IP 140.113.38.11 address. Redistribution subject to ECS terms of use (see ecsdl.org/site/terms_use) unless CC License in place (see abstract).

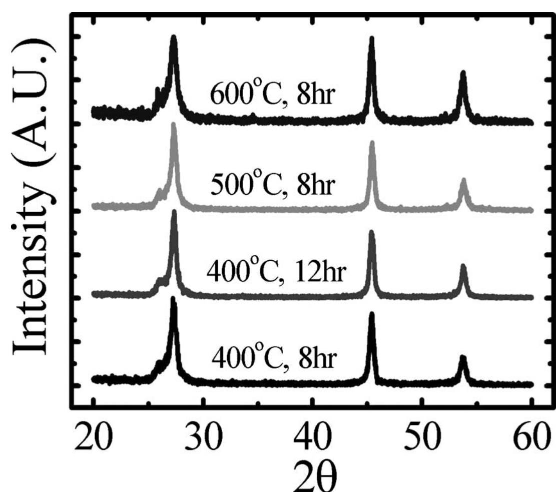

Figure 7. XRD patterns of the as-deposited Ge film capped with a SiN_x layer and of the samples obtained after recrystallization in a furnace for various lengths of time. The thicknesses of Ge films were ca. 160 nm.

GeO_x peak was nearly eliminated completely after annealing at higher temperatures. We suspected that the density of the Ge film would be improved after higher-temperature annealing and that the degree of surface oxidation would be reduced because of the higher density of the recrystallized Ge film. Table I summarizes the grain sizes, calculated using Scherrer's formula, of the Ge films treated with the various different recrystallization methods. Figure 9 displays the variation in surface roughness of the recrystallized Ge films as a function of the RTA temperature. The capping SiN_x layer would be removed by buffer-oxide-etch solution and then sent to AFM measurements. The surface roughness of recrystallized Ge films initially decreased after annealing at 600°C because of the smaller grains, but then increased after annealing at temperatures >700°C as the grains grew. Nevertheless, the root mean square values of the surface roughness remained small for all of the samples. Although larger grains could be obtained after annealing at 800°C (Fig. 10), some voids were also formed as a result of the decomposition of GeO_x units. In summary, the use of a capping SiN_x layer suppressed GeO_x formation during the densification and the use of RTA methods enhanced the crystallinity and grain size of the deposited Ge films more efficiently.

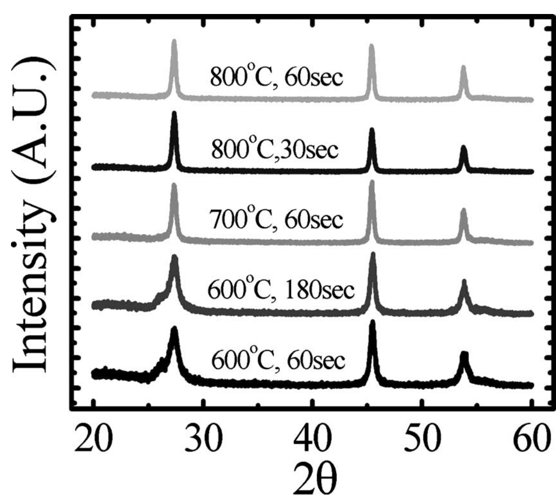

Figure 8. XRD patterns of the as-deposited Ge film capped with a SiN_x layer and of the samples obtained after recrystallization in a RTA system for various lengths of time. The thicknesses of Ge films were ca. 160 nm.

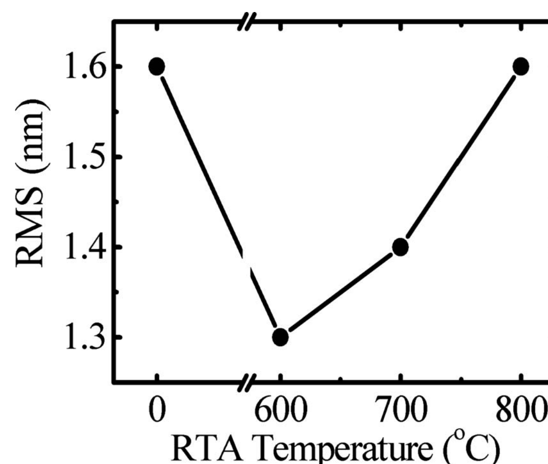

Figure 9. Variation of surface roughness of the recrystallized Ge films, which thicknesses were ca. 160 nm, plotted as a function of the RTA temperature. All the RTA process times were 60 s.

Electrical characteristics of the doped Ge film.— Figures 11a and b provide plots of the sheet resistance as a function of the RTA temperature for polycrystalline Ge (poly-Ge) and Si (poly-Si) films implanted with phosphorus and boron dopants, respectively. Prior to implantation, the poly-Ge films underwent RTA recrystallization (700°C, 60 s) in an N_2 ambient; the poly-Si films were subjected to furnace recrystallization (600°C, 24 h) in a N_2 ambient, i.e., under conditions used for poly-Si channel TFT devices. The RTA activation time for each of the samples after implantation was maintained constant at 60 s. For the n-type doped films, the sheet resistance of the implanted poly-Si films decreased as the RTA temperature increased, and the dopant became activated at temperatures of >600°C. In contrast, the sheet resistance of the implanted poly-Ge films increased initially but then decreased abruptly at temperatures

Table I. Grain sizes of the as-deposited Ge film capped with a SiN_x layer and of the samples obtained after recrystallization with the various recrystallization methods, various annealing temperatures, and for various lengths of time. The thicknesses of Ge films were ca. 160 nm.

Furnace orientation	300°C deposited	400°C 4 h (nm)	400°C 8 h (nm)	400°C 12 h (nm)	500°C 8 h (nm)	600°C 8 h (nm)
(111)	9.3	15.1	12.6	13.2	14.6	12.2
(220)	18.7	19.1	19.6	20.5	20.0	20.0
(311)	13.7	15.9	15.6	16.8	15.4	15.9
RTA orientation	**300°C deposited (nm)**	**600°C 60 s (nm)**	**600°C 180 s (nm)**	**700°C 60 s (nm)**	**800°C 30 s (nm)**	**800°C 60 s (nm)**
(111)	9.3	8.8	11.2	18.2	19.5	20.4
(220)	18.7	16.9	17.9	22.7	23.9	23.9
(311)	13.7	13.3	13.9	21.2	21.7	22.8

Downloaded on 2014-04-25 to IP 140.113.38.11 address. Redistribution subject to ECS terms of use (see ecsdl.org/site/terms_use) unless CC License in place (see abstract).

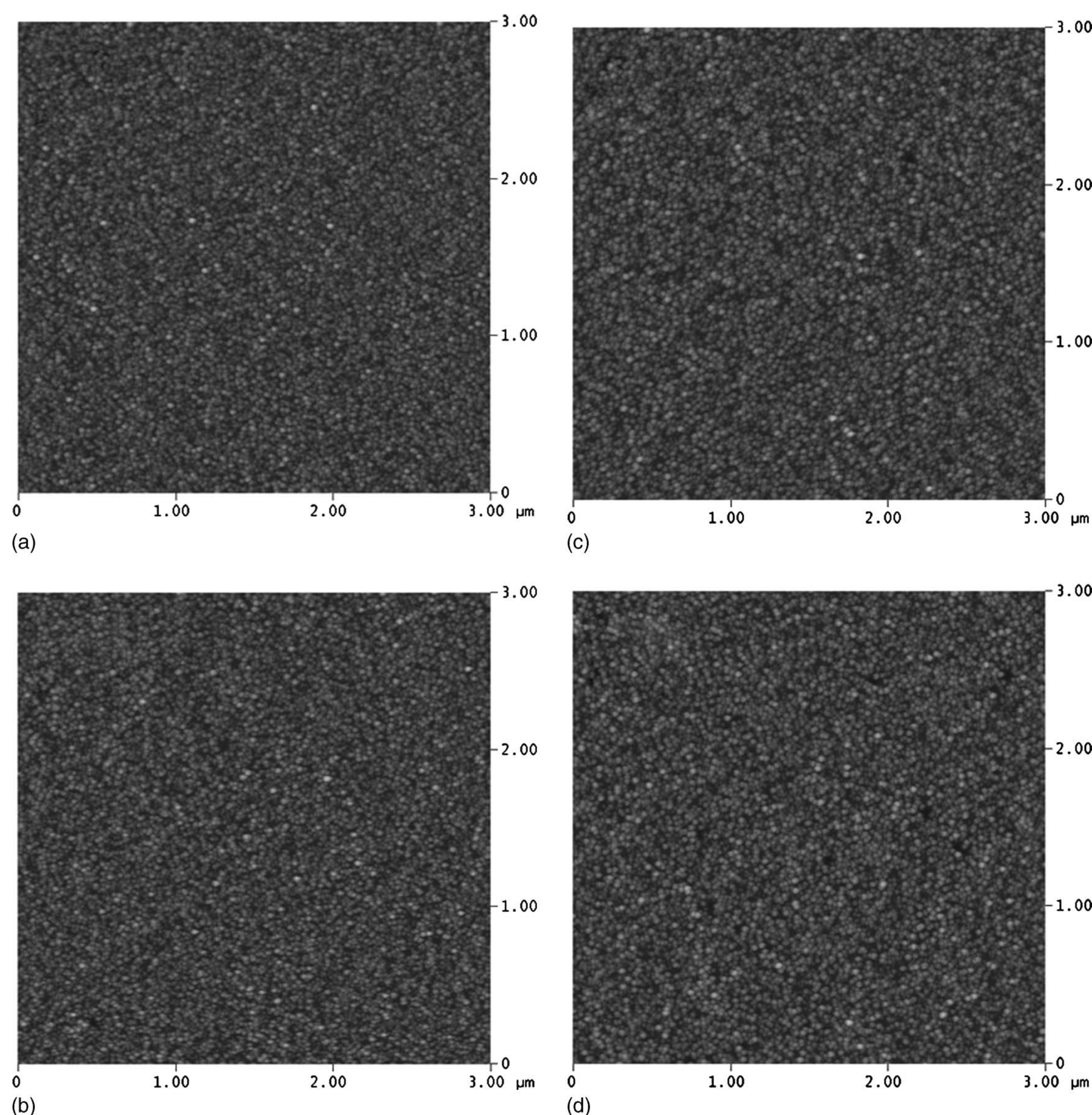

Figure 10. AFM images of the Ge films obtained after RTA treatment: (a) 600°C, 60 s; (b) 700°C, 60 s; (c) 800°C, 30 s; (d) 800°C, 60 s.

>500°C. The minimum sheet resistance of the poly-Ge films (231 Ω/□) was obtained at an annealing temperature of 550°C; the sheet resistance increased on increasing the RTA temperature above 600°C. The activation behavior of phosphor and boron implants in Ge has been investigated widely.[25-29] The activation efficiency of phosphorus dopants is poor: only a small fraction of the implanted dosage can be activated after RTA treatment. Furthermore, the dopants exhibited rapid diffusion, which, in turn, leads to a significant loss of dopant in the Ge case. As a result, we suspect that the increased sheet resistance of the n-type dopants as the RTA temperature increased to >600°C was due to the decreased dose of activated dopant and the increased dose loss at higher annealing temperatures. In contrast to the behavior of phosphorus, a high proportion of boron is electrically active immediately after implantation and it undergoes negligible diffusion in Ge after annealing. As a result, the sheet resistances for the p-type doped poly-Ge and poly-Si films exhibited similar trends. The implanted poly-Ge films were activated at 500°C and reached the minimum sheet resistance (105 Ω/□) at 550°C. There was only a slight increase in the sheet resistance when the annealing temperature was increased up to 750°C; this behavior might also be related to loss of the dopant when the annealing temperature was high. These results indicate that a low thermal budget is required for activation of the dopant, which seems to be very suitable for the fabrication of TFT devices on glass substrates.

Conclusion

We have investigated the physical and electrical properties of Ge films deposited directly using ICP-CVD techniques onto SiO_2-covered Si substrates. The deposition of very pure Ge thin films was achieved at 300°C without significant incorporation of O and C atoms. The mechanism of deposition was consistent with a hydrogen etching effect. Recrystallization in an RTA system rapidly improved the quality and smoothness of the Ge films. As a result, the adaptable sheet resistance of the poly-Ge films could be achieved at lower activation temperatures, making them more suitable for use in TFT device fabrication processes.

Acknowledgment

We thank the National Science Council, Republic of China (contract no. 95A0501), for its support.

National Nano Device Laboratories assisted in meeting the publication costs of this article.

Downloaded on 2014-04-25 to IP 140.113.38.11 address. Redistribution subject to ECS terms of use (see ecsdl.org/site/terms_use) unless CC License in place (see abstract).

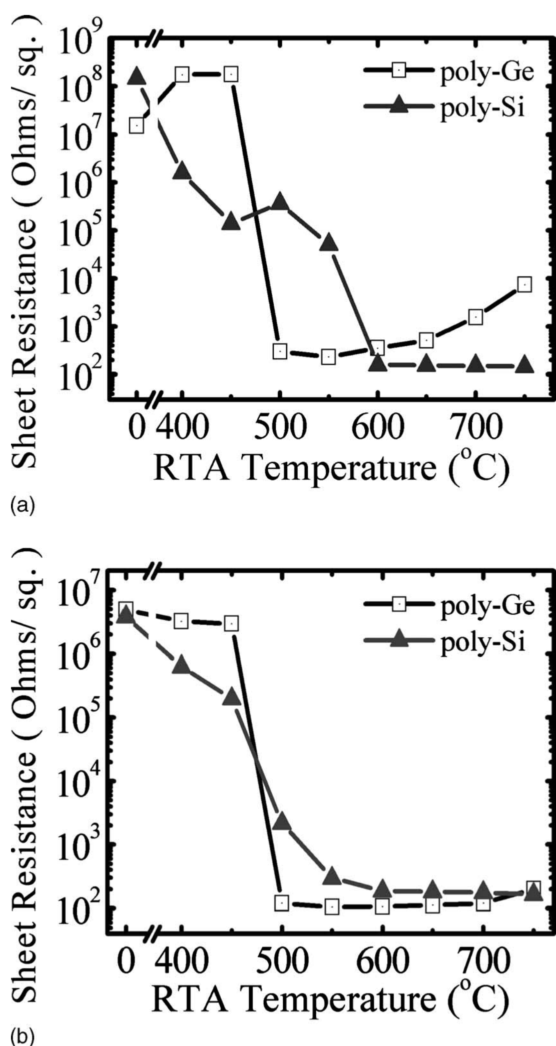

Figure 11. Sheet resistances plotted as a function of the RTA temperature for implanted poly-Ge and poly-Si films incorporating (a) phosphorus and (b) boron dopants.

References

1. H. Jorke and H. J. Herzog, *J. Electrochem. Soc.*, **133**, 998 (1986).
2. H. Shinoda, M. Kosaka, J. Kojima, H. Ikeda, S. Zaima, and Y. Yasuda, *Appl. Surf. Sci.*, **100–101**, 526 (1996).
3. C. O. Chui, S. Ramanathan, B. B. Triplett, P. C. McIntyre, and K. C. Saraswat, *IEEE Electron Device Lett.*, **23**, 473 (2002).
4. W. P. Bai, N. Lu, J. Liu, A. Ramirez, D. L. Kwong, D. Wristers, A. Ritenour, L. Lee, and D. Antoniadis, *2003 Symposium on VLSI Technology, Digest of Technical Papers*, p. 121, IEEE, June 10–12, Kyoto, Japan (2003).
5. H. Shang, H. Okorn-Schimdt, J. Ott, P. Kozlowski, S. Steen, E. C. Jones, H.-S. P. Wong, and W. Hanesch, *IEEE Electron Device Lett.*, **24**, 242 (2003).
6. H. Hibino, N. Shimizu, and Y. Shinoda, *J. Vac. Sci. Technol. A*, **11**, 2458 (1993).
7. C. H. Huang, M. Y. Yang, A. Chin, W. J. Chen, C. X. Zhu, B. J. Cho, M.-F. Li, and D. L. Kwong, *2003 Symposium on VLSI Technology, Digest of Technical Papers*, p. 119, IEEE, June 10–12, Kyoto, Japan (2003).
8. S.-I. Takagi, *2003 Symposium on VLSI Technology, Digest of Technical Papers*, p. 115, IEEE, June 10–12, Kyoto, Japan (2003).
9. T. Sadoh, H. Kamizuru, A. Kenjo, and M. Miyao, *Appl. Phys. Lett.*, **89**, 192114 (2006).
10. D. Dentel, J. L. Bischoff, T. Angot, and L. Kubler, *Surf. Sci.*, **402–404**, 211 (1998).
11. M. Okada, A. Muto, I. Suzumura, H. Ikeda, S. Zaima, and Y. Yasuda, *Jpn. J. Appl. Phys., Part 1*, (no. 12B), **37**, 6970 (1998).
12. Q. Li, S. M. Han, S. R. J. Brueck, S. Hersee, Y. B. Jiang, and H. Xu, *Appl. Phys. Lett.*, **83**, 5032 (2003).
13. S. Kobayashi, M. Sakuraba, T. Matsuura, J. Murota, and N. Mikoshiba, *J. Cryst. Growth*, **174**, 686 (1997).
14. M. Racanelli and D. W. Greve, *Appl. Phys. Lett.*, **58**, 2096 (1991).
15. T. Baron, B. Pelissier, L. Perniola, F. Mazen, J. M. Hartmann, and G. Rolland, *Appl. Phys. Lett.*, **83**, 1444 (2003).
16. Y. Liu, M. D. Deal, and J. D. Plummer, *Appl. Phys. Lett.*, **84**, 2563 (2004).
17. K. Egami and A. Ogura, *Appl. Phys. Lett.*, **47**, 1059 (1985).
18. D. Shahrjerdi, B. Hekmatshoar, S. Mohajerzadeh, and S. Darbari, *ICM 2003*, Cairo, pp. 361–364, Dec. 9–11, 2003.
19. J. L. Xu, J. L. Chen, and J. Y. Feng, *Nucl. Instrum. Methods Phys. Res. B*, **194**, 297 (2002).
20. M.-J. Yang, J. Shieh, S.-L. Hsu, I.-J. Huang, C.-C. Leu, S.-W. Shen, T.-Y. Huang, P. Lehnen, and C.-H. Chien, *Electrochem. Solid-State Lett.*, **8**, C74 (2005).
21. H. Ishii, Y. Takahashi, and J. Murota, *Appl. Phys. Lett.*, **47**, 863 (1985).
22. J. Hanna and K. Shimizu, *J. Organomet. Chem.*, **611**, 531 (2000).
23. T. Matsuura, T. Ohmi, J. Murota, and S. Ono, *Appl. Phys. Lett.*, **61**, 2908 (1992).
24. B.-T. Lee, T. R. Hayes, P. M. Thomas, R. Pawelek, and P. F. Sciortino, Jr., *Appl. Phys. Lett.*, **63**, 3170 (1993).
25. C. H. Poon, L. S. Tan, B. J. Cho, and A. Y. Du, *J. Electrochem. Soc.*, **152**, G895 (2005).
26. A. Satta, E. Simoen, R. Duffy, T. Janssens, T. Clarysse, A. Benedetti, M. Meuris, and W. Vandervorst, *Appl. Phys. Lett.*, **88**, 162118 (2006).
27. B. J. Pawlak, R. Surdeanu, B. Colombeau, A. J. Smith, N. E. B. Cowern, R. Lindsay, W. Vandervorst, B. Brijs, O. Richard, and F. Cristiano, *Appl. Phys. Lett.*, **84**, 2055 (2004).
28. Y. S. Suh, M. S. Carroll, R. A. Levy, G. Bisognin, D. De Salvador, M. A. Sahiner, and C. A. King, *IEEE Trans. Electron Devices*, **52**, 2416 (2005).
29. Q. Zhang, J. Huang, N. Wu, G. Chen, M. Hong, L. K. Bera, and C. Zhu, *IEEE Trans. Electron Devices*, **27**, 728 (2006).

Downloaded on 2014-04-25 to IP 140.113.38.11 address. Redistribution subject to ECS terms of use (see ecsdl.org/site/terms_use) unless CC License in place (see abstract).